ARTICLE

Received 00th January 20xx, Accepted 00th January 20xx

DOI: 10.1039/x0xx00000x

H/D Exchange Under Mild Conditions in Arenes and Unactivated Alkanes with C_6D_6 and D_2O Using Rigid, Electron-rich Iridium PCP Pincer Complexes

Joel D. Smith, a George Durrant, Daniel H. Ess Benjamin S. Gelfand and Warren E. Piers **

The synthesis and characterization of an iridium polyhydride complex ($Ir-H_4$) supported by an electron-rich PCP framework is described. This complex readily loses molecular hydrogen allowing for rapid room temperature hydrogen isotope exchange (HIE) at the hydridic positions and the α -C-H site of the ligand with deuterated solvents such as benzene-d₆, toluene-d₈ and THF-d₈. The removal of 1-2 equivalents of molecular H₂ forms unsaturated iridium carbene trihydride ($Ir-H_3$) or monohydride (Ir-H) compounds that are able to create further unsaturation by reversibly transferring a hydride to the ligand carbene carbon. These species are highly active hydrogen isotope exchange (HIE) catalysts using C₆D₆ or D₂O as deuterium sources for the deuteration of a variety of substrates. By modifying conditions to influence the $Ir-H_n$ speciation, deuteration levels can range from near exhaustive to selective only for sterically accessible sites. Preparative level deuterations of select substrates were performed allowing for procurement of >95% deuterated compounds in excellent isolated yields; the catalyst can be regenerated by treatment of residues with H₂ and is still active for further reactions.

Introduction

Metal-catalyzed hydrogen isotope exchange (HIE) is a key fundamental process for preparing isotopically labeled organic compounds necessary for studying reaction mechanisms and biological metabolic processes. Since the seminal work on homogeneous HIE by Garnett and Hodges^{2, 3} as well as Shilov and co-workers,^{4, 5} advances in analytical biology and chemistry have created an ever growing demand for deuterium⁶ and tritium⁷ labeled molecules.8 Consequently, an important body of research devoted to studying the homogeneously catalyzed exchange of hydrogen and deuterium atoms (H/D exchange) has developed over the last 25 years.9-12 by Bergman group Pioneering work the pentamethylcyclopentadienyl supported iridium hydrides demonstrated low temperature C-H activation 13-15 and it was subsequently shown that mild H/D exchange by cationic iridium complexes¹⁶⁻¹⁸ occurred under relatively mild conditions using C₆D₆ as a deuterium source. Most of these transformations involved selective deuterium incorporation into arene substrates^{10, 11} with only a handful

Tridentate "pincer" ligands have played a prominent role in homogeneous catalysis.^{25, 26} For example, polyhydridic pincer complexes of the late transition metals (particularly Ru and Ir) are known to be exemplary alkane dehydrogenation²⁷ and CO₂ reduction catalysts,^{28, 29} but recent work has demonstrated their promise as competent catalysts for promoting homogenous H/D exchange. Leitner, Milstein and co-workers were the first to show that a Ru based PNP polyhydride, I Chart 1, could use C₆D₆ or D₂O for arene deuteration at 50°C.^{30, 31} Shortly after, Zhou and Hartwig revealed that the aliphatic iridium PCP polyhydride II could be used as a pre-catalyst to efficiently perform H/D exchange between olefins and C₆D₆ at room temperature without isomerization.32 Following these reports, PNP (III) and PCP (IV) complexes synthesized by Grubbs³³ and Wendt³⁴, respectively, were also tested as HIE mediators. The iridium dihydride species III was able to selectively deuterate aromatic compounds and silanes, while the cyclohexyl-based PCP complex IV was found to successfully deuterate arenes and to a limited extent C_{sp3}-H sites, albeit at elevated temperatures of 150 °C.

Design elements of the ligands II/IV and III have been incorporated into a family of PCP ligands V introduced by our group³⁵ and also explored by others. ³⁶⁻³⁹ An attractive feature of these ligands is their ability to assume $PC_{sp3}P$ or $PC_{carbene}P$ forms by the addition or removal of a hydrogen atom from the anchoring carbon of the pincer framework. This has precedence in the ligands II and IV but in the aryl-

Electronic Supplementary Information (ESI) available: Synthesis, characterization data, experimental and computational details. Crystallographic data for [Ir-H₄ and Ir-Ph (CCDC numbers: 2002787-2002788) in the form of .cif files. See DOI: 10.1039/x0xx00000x

of catalysts capable of H/D exchange on unactivated alkane substrates under more forcing conditions. 16, 17, 19-24

^{a.a} Department of Chemistry, University of Calgary, 2500 University Drive NW, Calgary, Alberta T2N 1N4, Canada.

b. Department of Chemistry and Biochemistry, Brigham Young University, Provo, Utah 84602, USA

ARTICLE

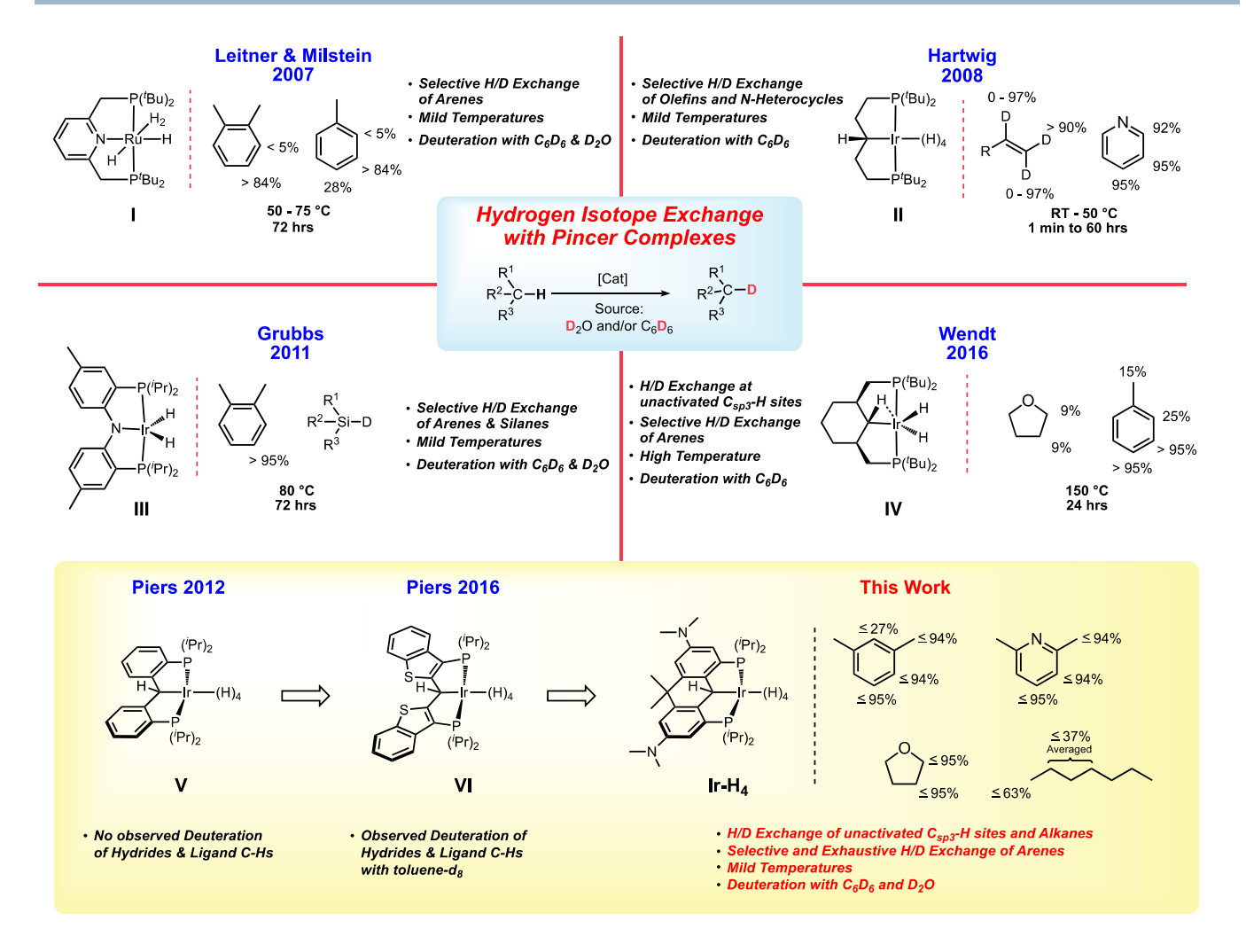


Chart 1 Contextualization of this study.

linked PCP systems **V** (and the related benzothiophene-based system VI^{40}) this is potentially more controllable because of the lack of β -hydrogens in the PCP linker framework, and through manipulation of the electronic properties of the ligand via substitution on the aryl linkers and/or rigidification of the ligand via additional linking of the backbone aryl groups. A1, A2 With these two structural levers, a library of PCP ligands has been prepared and a substantial range of CO concluses has been found for CO [(PCcarbeneP)IrCO]+ species. We have shown that the rate of addition of CO to the C=Ir bond Can therefore be tuned substantially. Furthermore, the rigidification of the ligand tends to favor the CO corresponded from of the ligand vs. the CO bond cleavage reactions that destroy the integrity of

the ligand in unlinked systems akin to **V**.⁴⁵ The ability of the carbon atom in these PCP pincers to engage in ligand cooperativity has been exploited in hydrogen,^{35, 46} silane⁴⁷⁻⁴⁹ and other small molecule^{40, 50-53} activations in various systems. Furthermore, in polyhydridic systems, the dibenzylic hydrogen is actively involved in exchange with the metal hydrides,^{34, 35} increasing the "hydrogen capacity" of these compounds relative to other (for example PNP) polyhydridic pincer complexes and potentially providing new pathways for catalysis.

In both the parent, unsubstituted, unlinked system V,³⁵ and that incorporating the benzothiophene-based ligand VI,⁴⁶ the Ir polyhydride is only stable under an atmosphere of dihydrogen but it was observed that slow H/D exchange in the sterically exposed C-H bonds of the ligand aryl

backbone occurred in C_6D_6 . We hypothesized that a more electron rich system would accelerate this process and indeed, the linked dihydroanthracene PCP ligand framework fitted with electron donating dimethylamino groups para to the PCP carbon (bottom of Chart 1) supports a stable, isolable polyhydride species $Ir-H_4$ (Chart 1). While stable as a solid, this complex readily loses molecular hydrogen in solution to give species that are highly active HIE catalysts at low loadings and under mild conditions. Both C_6D_6 and D_2O can be used as deuterium sources and selectivity can be modulated to some extent by controlling the catalyst speciation.

Results and Discussion

Synthesis and Characterization of Iridium PCP Pincer Polyhydride Ir-H₄.

Using methodology established previously, $^{46, 54}$ the iridium PCP pincer complex **Ir-OH** was prepared by heating the previously reported **Ir-Cl**⁴⁴ to 120 °C in toluene with an excess of CsOH for 24 hours (Scheme 1, red arrows). The resulting brown solution was filtered through Celite® and a brown powder was isolated in 80% yield after removing all volatiles *in vacuo*. The **Ir-OH** complex displays a characteristic -OH triplet ($^3J_{HP} = 3.8 \text{ Hz}$) at 3.62 ppm in the 1H NMR spectrum as well as a singlet in the $^{31}P\{^1H\}$ NMR at 51.9 ppm. The presence of an iridium-carbene moiety was indicated by a triplet signal at 196.0 ppm ($^2J_{CP} = 2.2 \text{ Hz}$) in the $^{13}C\{^1H\}$ NMR spectrum.

Scheme 1. Synthetic routes to iridium PCP polyhydride Ir-H₄

Dissolving **Ir-OH** in benzene and exposing it to 4 atm. of H_2 gas for 3 hours resulted in a color change from dark reddish-brown to yellow-orange. The $^{31}P\{^1H\}$ NMR spectrum for the solution exhibited a single peak at 56.5 ppm and upon solvent removal a brown residue was formed. This residue was then stirred in *n*-pentane under 1 atm. of H_2 for 20 minutes producing a beige powder, **Ir-H**₄, that was isolated in 98% yield following the removal of all

volatiles in vacuo. Alternatively, we found stirring the precursor Ir-Cl with NaOH (10 eq.) under H₂ gas (4 atm.) in benzene for 3 hours produced a similar red-orange solution (Scheme 1, blue arrow). Following filtration through a pad of Celite®, the solution was stirred for 20 minutes under H₂ gas. All volatiles were removed in vacuo and a beige powder was again isolated in 94% yield. Compared to the parent ortho-phenylene V35 (Chart 1) and the benzothiophene-based ligand congener VI,46 which both could not be isolated due to decomposition via loss of H₂ under vacuum, complex Ir-H₄ is remarkably stable as a solid and can be stored indefinitely at room temperature under an inert atmosphere. Furthermore, it can be interrogated NMR spectroscopy in cyclohexane-d₁₂ methylcyclohexane- d_{14} under argon, whereas the others (V and VI) must be kept under an atmosphere of H2 in order to avoid decomposition. The ¹H NMR spectrum for Ir-H₄ in cyclohexane- d_{12} displays a single triplet (average $J_{HP} = 10.2$ Hz) resonance at -10.32 ppm and a singlet at 5.52 ppm, integration indicating the presence four rapidly exchanging hydridric nuclei and one α -C(H)-Ir proton, respectively. Moreover, the ligand resonances in the spectrum clearly point to C_s symmetry with 12 equivalent dimethyl amino protons represented by a singlet at 2.85 ppm and two signals at 1.23 ppm and 1.84 ppm for the inequivalent -CH₃ groups attached to the carbon backbone linker. The ¹³C(¹H) NMR also corroborates the formation of Ir-H₄ showing the loss of the carbene triplet associated with the Ir-Cl and Ir-OH complexes and the presence of a signal at 21.0 ppm coupling to the α -C-H proton at 5.52 ppm in the $^1\text{H}-^{13}\text{C}$ HSQC spectrum.

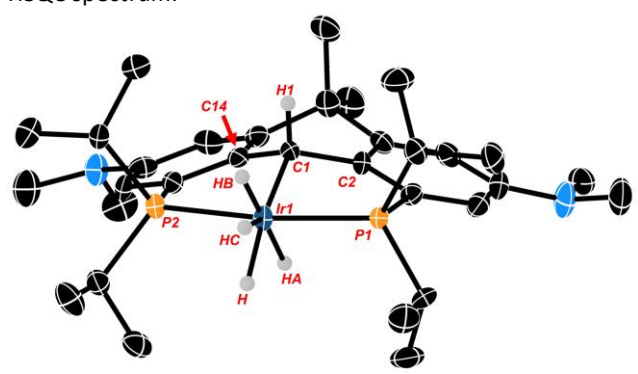
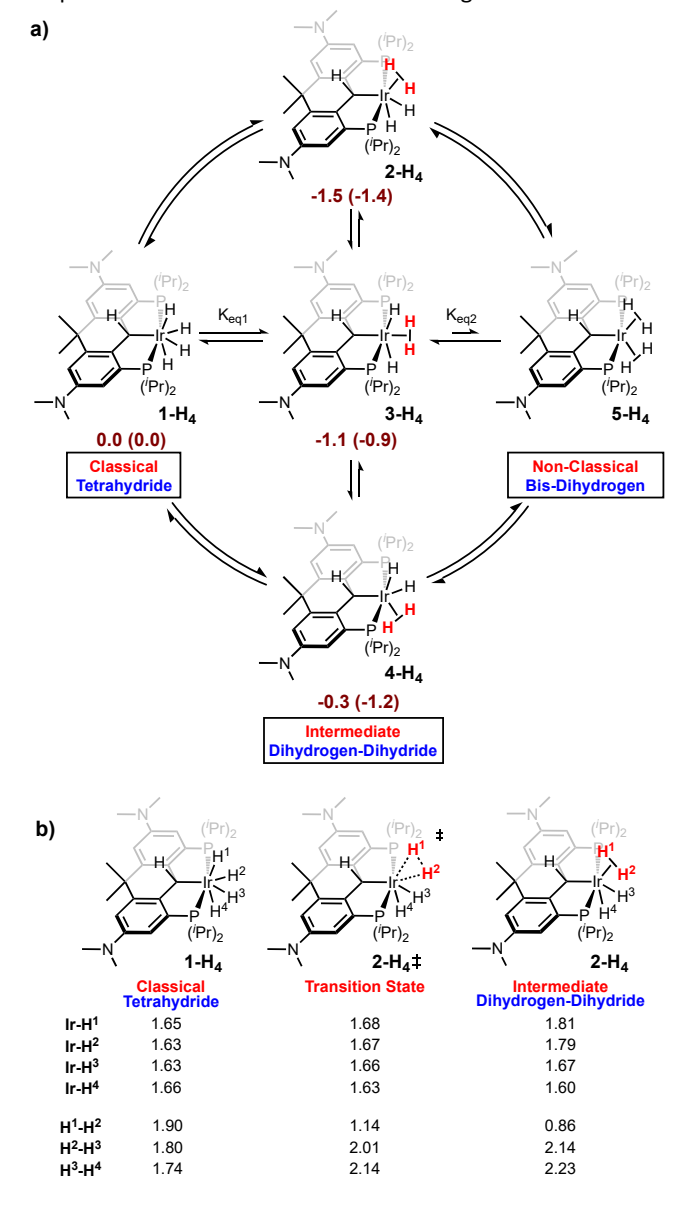


Figure 1. Thermal ellipsoid diagram of Ir-H₄ (ellipsoids drawn to 50 % probability; all hydrogen atoms except H, H1, HA, HB and HC have been omitted for clarity). Selected metrical data for Ir-H₄: Bond distances (Å); Ir1-C1, 2.186(5); Ir1-P1, 2.2703(16); Ir1-P2, 2.2786(16), C1-C2, 1.496(8); C1-C14 1.519(8). Bond Angles (°); P1-Ir1-P2, 163.45(5); Ir1-C1-C2, 112.9(4); Ir1-C1-C14, 112.0(4); C2- C1-C14, 110.2(5).

Crystals of the compound were obtained by slowly cooling a supersaturated solution of $Ir-H_4$ in isopropanol from 50 °C to 20 °C and crystallographic analysis corroborates the solution data described above. Unfortunately, we were unable to locate the hydrogen atoms associated with the metal center directly within the Fourier map and cannot comment on the nature of their arrangement in the solid state. Nevertheless, the data show the anchoring α -carbon

(C1 in Figure 1) is pyramidalized (the sum of the angles about C1 is 335.2(8)°), and the central 6 membered ring containing this α -carbon has also adopted a "boat"-like conformation. The sp³ hybridization of the α -carbon is also indicated by the central Ir1-C1 bond length of 2.184(5) Å which is similar to other sp³ hybridized Ir-C bonds we have observed with these NR₂ substituted ligand frameworks^{44,45} and lengthened significantly from the values of \approx 1.93 Å seen in PC_{carbene}P complexes of this ligand.⁴⁴

Given the lack of crystallographic data concerning the iridium hydrides in Ir-H₄, we turned to criteria developed by Halpern and co-workers⁵⁵ to shed some light on what form



Scheme 2. a) Outline of isomerism in Ir-H₄ with benzene-solvated enthalpies (Gibbs energies) in kcal/mol. b) Ir-H and H-H distances (Å) found in M06 DFT structures

dominates the speciation of $Ir-H_4$ in solution. While it is typically difficult to unambiguously categorize the hydride bonding mode for these complexes, we were able to rule out the possibility that $Ir-H_4$ is a "non-classical" Ir(I) bis-

dihydrogen species (Scheme 2). The T₁(min) relaxation for the hydridic nuclei of $Ir-H_4$ in methylcyclohexane- d_{14} (Figure S1) was found to be 186 ms at 600 MHz (10 °C \pm 0.5 °C), approximately 155 ms when adjusting to a 500 MHz field strength. These values are comparable to those obtained for other PCP pincer polyhydride complexes reported by Heinekey,⁵⁶ Wendt³⁴ and us;³⁵ a collection of comparative data is given in Table S1. The data point to an equilibrating mixture of a "classical" Ir(V) tetrahydride and the "intermediate" Ir(III) dihydrogen-dihydride isomers shown. The experimental T₁ of 155 ms is somewhat lower than the calculated T_1 value of 203 ms calculated from the parameters obtained from the M06 density functional theory (DFT) optimized structure of Ir-H₄, suggesting a significant contribution from any or all of the dihydrogendihydride isomers, which also can be optimized using DFT and give rise to T_1 values of \approx 15 ms using the Halpern methodologies. Significantly, the non-classical bisdihydrogen structure could not be optimized by DFT, suggesting that this formally Ir(I) isomer is not favored with this electron rich pincer ligand and does not contribute to the speciation of Ir-H₄ in solution.

Another key metric in this family of compounds is the averaged J_{H-D} coupling constant in the Ir-HD₃ isotopologue. For Ir-H₄, this species is trivially prepared by dissolving Ir-H₄ in C₆D₆ and stirring for 15 minutes at room temperature (vide infra), removing the solvent and redissolving the sample in methylcyclohexane- d_{14} . All four iridium hydrides and the benzylic position on the ligand are rapidly deuterated under these conditions, but by halting before full deuteration, the residual hydride resonance in methylcyclohexane- d_{14} at -10.25 ppm displays a resolved seven line pattern with an average observed J_{H-D} of 3.1 ± 0.1 Hz when collected at 50 °C (Figure S2). This coupling correlates to an approximated average H-H atomic distance of 1.02-1.25 Å (Table S1),56 and is consistent with equilibrating classical tetrahydride (H-H > 1.2 Å) and intermediate dihydrogen (H-H ≈ 1.0-1.2 Å) dihydride structures (Table S1)57-59 as depicted in Scheme 2. Unlike the related system based on IV, attempts to freeze out the exchange between the isomers of the latter and/or the equilibrium between the two via variable temperature ¹H{³¹P} NMR spectroscopy on Ir-H₄ in methylcyclohexane d_{14} showed no decoalescence of the hydride resonance to temperatures as low as -110 °C (Figure S3). This indicates a lower energetic barrier for hydride exchange than the estimated 8.7 kcal/mol at -70 °C reported by Wendt et al. in the system IV.34 Indeed, M06 DFT calculations indicate the potential energy surface for postulated tetrahydride and dihydrogen-dihydride complexes is relatively flat with an energy range of < 2 kcal/mol between these four structures (Scheme 2). For the full covalent Ir-H bonds, the distances are ~1.6 Å. In the dihydrogen-dihydride structures, the dihydrogen distances are ~0.85 Å, which are only slightly stretched compared to free H_2 .⁵⁹ The barriers are < 12 kcal/mol for conversion between tetrahydride and dihydrogen-dihydride complexes. The transition-state

distances for the forming H-H bonds are ~1.1 Å. Overall, these DFT thermodynamic and kinetic estimates suggest that all intermediate and classical structures are accessible in solution and the spectroscopically observed complex lies within the dihydrogen-dihydride tetrahydride continuum. While the benzylic hydrogen on the $C_{\rm sp3}$ carbon of the ligand certainly exchanges with the four iridium hydrogens rapidly on the chemical timescale, the two peaks only undergo slight broadening at temperatures below which loss of H_2 and conversion to other species ensues (*vide infra*). Line shape analysis to probe the barrier was not possible with the spectral data available in this system, unlike that of $IV.^{34}$

Scheme 3. Solution chemistry of Ir-H₄.

Solution Behavior of Ir-H₄.

While $Ir-H_4$ is quite stable in the solid state, evidence exists for reversible loss of H_2 in solution (Scheme 3). When dilute solutions in benzene were exposed to vacuum, the pale-yellow color darkened slowly to a maroon-tinged hue. Readmission of H_2 gas to the vessel gave back the yellow

solution; monitoring this transformation by NMR spectroscopy indicated that the maroon solution was essentially spectroscopically identical to the yellow solutions of Ir-H₄. However, when heating solutions of Ir-H₄ to 80 °C under a static vacuum and monitoring by NMR spectroscopy, other resonances became apparent. In the ¹H NMR spectrum, a new resonance at 2.71 ppm in the NMe₂ region and a faint peak at -10.30 ppm were observed in about a 12:3 ratio. In the 31P{1H} NMR spectrum, resonance at 66.4 ppm grew in relative to that of Ir-H₄ at 56.5 ppm (Scheme 3, Figures S4 and S5). Cooling the sample resulted in loss of this resonance and a return to solutions that were >98% Ir-H₄. We hypothesized that this maroon species was either the PC_{sp3}P supported Ir(III) dihydride Ir-H₂ or the PCcarbeneP ligated Ir(III) trihydride Ir-H₃ shown in Scheme 3. These should be distinguishable by the ¹³C resonance of the PCP ligand, but because it is produced in such small amounts via this method, we sought ways to prepare or at least enrich the speciation of this compound in order to obtain more concentrated samples.

Heating in benzene under dynamic vacuum did lead to a much darker colored solution, but the ³¹P{¹H} NMR spectra indicated that a third species with a resonance at 53.6 ppm was dominant in these samples. Separate synthesis, NMR spectroscopy and X-ray crystallography confirmed this product to be the PCcarbeneP Ir(I) phenyl complex Ir-Ph (Scheme 3). In attempts to generate Ir-H₂/Ir-H₃ by treating Ir-H₄ with the dehydrogenation agent tert-butyl ethylene, varying mixtures of the three components were obtained depending on the equivalency of olefin employed; when > 3 equivalents were used, Ir-Ph was cleanly produced and isolated as a green solid in 72% yield. The ¹³C{¹H} NMR spectrum of Ir-Ph in benzene- d_6 shows a distinct carbene triplet at 221.1 ppm ($J_{CP} = 4.2 \text{ Hz}$) while the ¹H NMR spectrum shows three separate aryl proton signals for the new phenyl group as well as characteristic ligand resonances. Crystallographic data (Figure 2) show a central Ir1-C1 distance of 1.965(4) Å. This is shorter than that found in Ir-H₄ and indicative of an iridium carbene bond similar to analogous structures. 35, 40, 43-45 Accordingly, unlike the boatlike shape found in the Ir-H4 the central 6-membered ring of the ligand framework in Ir-Ph adopts a planar conformation, as a result of the sp² hybridization found at the carbene center. The rigidity of the ligand employed here stabilizes this phenyl complex with respect to the intriguing C-C bond formation reaction observed by Wendt in a the more flexible IV.60

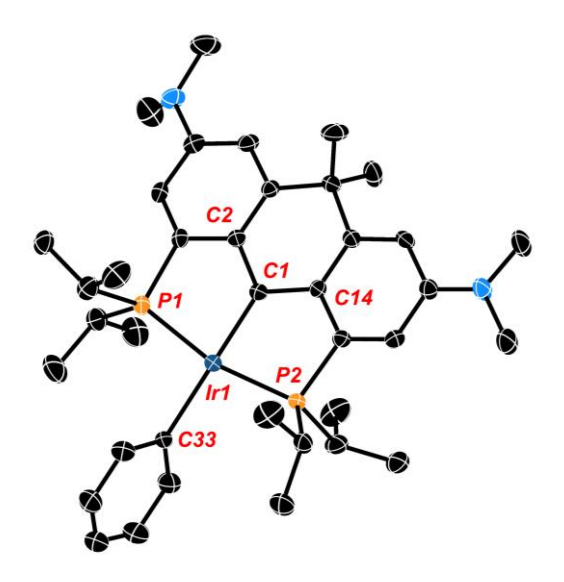


Figure 2. Synthesis and thermal ellipsoid diagram of **Ir-Ph** (ellipsoids drawn to 50% probability; hydrogen atoms have been omitted for clarity). Selected metrical data for **Ir-Ph**: Bond Distances (Å): Ir1-C1, 1.965 (4); Ir-C33, 2.118(4); Ir1-P1, 2.2581(13); Ir1-P2, 2.2671(17), C1-C2, 1.467(6); C1-C14 1.469(6). Bond Angles (9); P1-Ir1-P2, 166.46(4); C1-Ir1-C33, 179.53(19); P1-Ir1-C1, 83.46(13); P1-Ir1-C33, 96.38(13); Ir1-C1-C2, 122.6(3); Ir1-C1-C14, 122.9(4); C2-C1-C14, 114.5(4).

Taken together, the above observations suggest that Ir-H4 rather easily loses one equivalent of H2, even thermally, to give Ir-H₂/Ir-H₃, but when exposed to vacuum and heat, a second equivalent of H2 is eliminated to form the (unobserved) compounds Ir-[]/Ir-H depicted in Scheme 3. Consistent with the relative ease for H2 loss, the DFT calculated energy of Ir-H₃ is only endergonic by ~5 kcal/mol relative to Ir-H₄. Calculations suggest that formation of the dihydrogen-dihydride complex and dihydrogen dissociation is required before 1,2-hydrogen shift from the ligand to Ir to form Ir-H₃, which only requires a barrier of ~15 kcal/mol. The Ir-H Ir-[] structures are calculated to be 6.6 and 12.2 endergonic relative to Ir-H₄. Overall, the thermodynamic and kinetic DFT calculations suggest that Ir-H₃, Ir-H₂, Ir-H, and Ir-[] structures are all viable. These compounds rapidly C-H activate benzene and, after elimination of another equivalent of H2, Ir-Ph is produced; this compound rapidly converts back to Ir-H₄ upon treatment with H₂, with loss of C₆H₆. The speciation of the Ir-H₂/Ir-H₃ manifold was solidified as being mainly Ir-H₃ by mixing isolated Ir-H₄ and Ir-Ph in a ≈ 2:3 ratio in benzene; this experiment resulted in an equilibrium mixture of these two compounds along with about 40% Ir-H₃ which allowed us to acquire meaningful ¹H and ¹³C NMR data on the latter. Both are consistent with C_{2v} symmetry and the presence of a $PC_{carbene}P$ ligand. In the ${}^{1}H$ NMR spectrum, no resonance in the region between 3 and 6 ppm consistent with the presence of an α -C(H)-Ir proton was observed, while a characteristic resonance at 245.0 ppm in the ¹³C{¹H} NMR spectrum is diagnostic of a carbene carbon. This signal correlated with the triplet integrating to 3 hydrogens at -10.12 ppm in the 2D ¹H-¹³C HMBC spectrum. At room temperature, the single resonance for

the three hydrides in Ir-H₃ indicate they are in rapid exchange, presumably via a 1,2-hydride shift from the iridium to the carbene carbon, *i.e.*, via Ir-H₂. The apparent thermodynamic preference for Ir-H₃ over Ir-H₂ in this system contrasts with observations reported by Wendt and co-workers,^{34, 61} but these structures are very close in energy and in rapid exchange. While DFT calculations using a variety of functionals (M06, wB97X-D, M11, and others) all indicate that the Ir-H₂ structure is slightly lower in energy than Ir-H₃, the methodology has limitations for distinguishing these types of isomers accurately.

HIE with Iridium Polyhydrides Ir-Hn.

As briefly alluded to above, dissolution of $Ir-H_4$ into C_6D_6 (and indeed toluene- d_8 or $THF-d_8$) leads to the rapid deuteration of the α -C(H)-Ir and Ir-H positions at 20 °C to form $Ir-D_4$ (Scheme 4a) and so it had to be characterized in deuterated cyclohexane or methylcyclohexane solvents which do not surrender deuterium at room temperature. Heating $Ir-H_4$ in C_6D_6 to 65 °C for 24 hours lead to trace deuteration of the ligand NMe_2 and iso-propyl methyl groups (Figure S6). Given the coordinative saturation of $Ir-H_4$, we hypothesized that hydrogen loss to form $Ir-H_3$ was required to initiate the HIE process. Indeed, mixing $Ir-H_4$ and Ir-Ph as described above to generate solutions

a)
$$N$$
 $(^{(P_r)_2}$ C_6D_6 $C_6H_nD_{6-n}$ $(^{(P_r)_2}$ C_6D_6 $C_6H_nD_{6-n}$ $(^{(P_r)_2}$ C_6D_6 $C_6H_nD_{6-n}$ C_6D_6 $C_6H_nD_{6-n}$ C_6D_6 $C_6D_$

b)
$$(Pr)_2$$
 $(Pr)_2$ $(Pr)_2$

Scheme 4. HIE in Ir-H₄.

ARTICLE

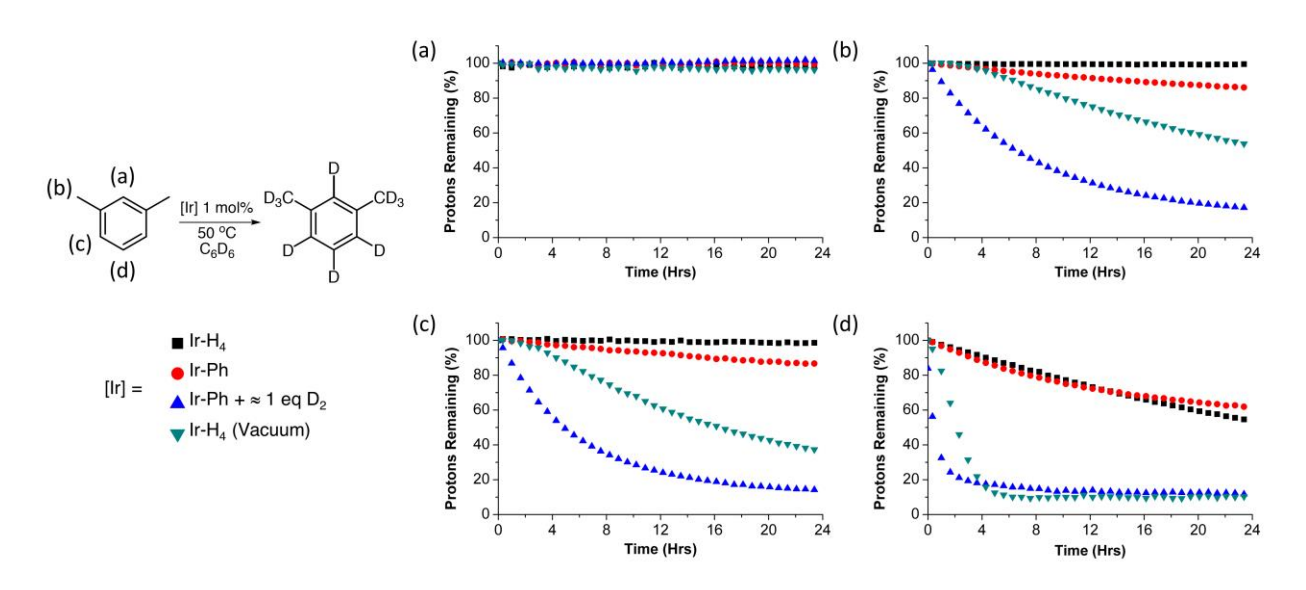


Figure 3. Reaction profiles of the H/D exchange at the 2 (graph a), benzyl (graph b), 4 and 6 (graph c) and 5 (graph d) position of m-xylene (0.38 mmol) in C_6D_6 (0.5 mL) using 1 mol% of either Ir-H₄ (black square), Ir-H₄ placed under static vacuum (green inverted triangle), Ir-Ph (red circle) or Ir-Ph activated with \approx 1 equivalent of D_2 gas (blue triangle). Conversion was measured via ¹H NMR using cyclooctane as an internal standard.

enriched in $Ir-H_3$ leads to much higher deuteration activity. Heating solutions of $Ir-H_4/Ir-H_3/Ir-Ph$ (3:2:2) in C_6D_6 to 65 °C for 24 hours gave the three species essentially exhaustively deuterated in the positions shown in Scheme 4b (Figure S7). Separate experiments showed that heating pure Ir-Ph under these conditions gave only 70% conversion to $Ir-Ph_{d5}$ after 24 hours and no deuteration of the ligand NMe_2 or *iso*-propyl groups was observed (Figure S8), suggesting that Ir-Ph is not an effective HIE promoter in this system.

While the Pr groups are likely deuterated via an intramolecular C-H activation, deuteration of the more remote NMe₂ groups suggest that intermolecular catalytic deuteration of other substrates under mild conditions might be possible. We chose meta-xylene as a test substrate to evaluate the various iridium species as HIE catalysts due to the sterically varied aryl C-H bonds present, as well as the benzylic sp³ hybridized C-H bonds. The results of these experiments are summarized in Figure 3. Solutions containing meta-xylene and 1 mol% of either Ir-H₄ (argon, 1 atm.), Ir-H4 (static vacuum), Ir-Ph (argon, 1 atm.) or Ir-Ph activated with D₂ gas (≈ 1 equivalent) were heated to 50 °C in benzene- d_6 and monitored by ¹H NMR spectroscopy. Each panel in Figure 3 indicates the rate of loss of substrate protons as time progresses for a different C-H position in the substrate, as a function of the catalyst precursor employed (colored shapes). Cyclooctane was employed as an internal standard. As can be seen in panel a, none of the catalyst formulations deuterate the sterically encumbered 2

position of meta-xylene at 50 °C; the other positions, however, are deuterated to varying degrees. In general, Ir-H₄ under argon and Ir-Ph behave similarly for deuteration of the C-H bonds in the benzylic, and aryl 4/5 positions, with moderate activity observed only for the sterically accessible aryl C-H bond in the 5 position. The catalyst systems which would be expected to generate Ir-[]/Ir-H, (Scheme 3) or Ir-H₂/Ir-H₃, namely Ir-Ph plus D₂ (blue triangles) or Ir-H₄ under vacuum (green inverted triangles) fared much better, with the former able to almost completely deuterate meta-xylene at all three positions under these mild conditions. Notably, when Ir-H₄ is simply exposed to vacuum (green triangles), there is an acceleration in the rate of deuteration consistent with the slow formation of Ir-H₃ through loss of H₂ to the headspace, whereas when the active species is generated through activation of Ir-Ph with D2, a more typical first order time evolution is observed, further implicating Ir-H₃ as the active catalyst or catalyst precursor.

Since it was clear from the above experiments that Ir-Ph activated with D_2 gave the most active HIE catalyst, further optimization of conditions for this reaction were undertaken with this as a starting point (Table 1). Entries 1 and 2 reaffirm that a catalyst is required, and that Ir-Ph itself is a poor catalyst with low activity. Entries 3-6 show that there is an optimal amount of added D_2 required to activate the catalyst of 1-3 equivalents. With excess D_2 (entry 7), activity drops off markedly, presumably because

the iridium speciation is now essentially 100% Ir-D₄, which (as shown in Figure 3) is not active under these conditions. Raising the temperature 15 degrees to 65 °C (entries 8-12) leads to greater HIE activity; comparison of entry 4 with entry 10 underscores this observation. Even the difficult 2-position sees some deuteration at this stage. As entries 11 and 12 show, near exhaustive deuteration of the benzylic, 4/6 and 5 positions can be achieved at 65 °C, with 1 mol% of Ir-Ph activated with 1.4 equivalents of D₂; entry 12 uses double the amount of C_6D_6 in order to drive the deuteration in these positions to near completion.

In comparison to other PCP (and PNP) pincer catalysts $^{\rm 31}$ for HIE reactions (Chart 1), the iridium systems described

 $\textbf{Table 1.} \ \, \textbf{Optimization of conditions for exhaustive deuteration of} \ \, \textit{meta-xylene with} \\ \ \, C_6D_6.$

5	benzyl 4/6	$\frac{\text{Ir-Ph } (1 \text{ mo } D_2)}{C_6 \textbf{D}_6}$	I%) →	D ₃ C	CD ₃		
Entry	Temp	D_2	Time	Position			
	(°C)	(mol%)	(hrs)	% deuterated (TOF, hr ⁻¹)			
				benzyl	2	4/6	5
1	50	No Cat.	24	0 (0)	0	0 (0)	0
2	50	0	3.5	3 (1)	0	2 (1)	11 (3)
3	50	1.0	3.5	31 (53)	0	40 (23)	77 (22)
4	50	1.4	3.5	32 (55)	0	41 (23)	81 (23)
5	50	1.8	3.5	26 (45)	0	34 (19)	82 (23)
6	50	3.0	3.5	23 (39)	0	33 (19)	87 (25)
7	50	9.0	3.5	0 (0)	0	0 (0)	8 (2)
8	65	9.0	3.5	0	0	0	20 (6)
9	65	9.0	24	0	0	6 (< 1)	70 (3)
10	65	1.4	3.5	69 (118)	4 (1)	77 (44)	88 (25)
11	65	1.4	24	89 (22)	13 (< 1)	91 (8)	89 (4)
12ª	65	1.4	24	94 (24)	27 (1)	95 (8)	95 (4)

Optimization performed with *meta*-xylene (0.38 mmol) and Ir-Ph (1 mol%) in C_6D_6 (0.5 mL). D_2 gas was injected into 0.015 M solutions of **Ir-Ph** in C_6D_6 and stirred for 10 minutes prior to its addition to *m*-xylene in C_6D_6 (0.25 mL). Conversion was measured *via* ^1H NMR using cyclohexane as an internal standard. $^a\text{Volume}$ of C_6D_6 increased to 1.0 mL.

here appear to be more active under milder conditions. Furthermore, through manipulation of the speciation of the active $Ir-H_n$ compounds, the selectivity of deuteration can also be to some extent controlled. Finally, given the stability of these systems to water, D_2O can also be used as a deuterium source rather than C_6D_6 . The results of HIE with

a number of substrates, under three sets of conditions are summarized in Figure 4.

Using the optimized conditions of Entry 11 in Table 1 developed for meta-xylene, HIE for several substrates were examined (Figure 4, black data). Deuterium incorporation was found to be quite high for several arene based substrates with unhindered C_{sp2-}H positions in fluorobenzene, naphthalene, aniline and 2,6-lutidine being In the case of deuterated almost quantitatively. naphthalene even the less reactive bay positions were fully deuterated in contrast to III33 and IV,34 which required longer reaction times and higher temperatures to achieve even partial deuteration of these positions in naphthalene. More interestingly, typically less active C_{sp3}-H positions were significantly deuterated in substrates such as THF, triethylamine, 2,6-lutidine and meta-xylene under very mild conditions with no sign of catalyst decomposition. This level of deuteration for the $C_{\text{sp3}}\text{-H}$ sites, along with precedents from previous systems, 17, 24, 62 prompted further investigation into the deuteration of aliphatic hydrocarbons. Despite no detectable H/D exchange occurring between benzene-d₆ and cyclooctane at 50 °C the increased temperature of 65 °C resulted in mild deuteration of 9% after 24 hours which increased to 36% after 5 days. For *n*-heptane, deuteration of the terminal methyl groups was found to be 58% while internal methylene positions were deuterated to 37% after 5 days. The ¹³C{¹H} NMR revealed that the majority of deuteration performed on the interior methylene groups occurred the 2 and 6 positions. This is intriguing considering reactivity of cyclopentadienyl Ru complex reported by Nikonov was limited to the terminal methyl C-H sites.²⁴ Reduced activity was also observed with phenol while catalysis was completely halted in the presence of ethyl benzoate and pyridine. The ³¹P{¹H} NMR spectra of these latter reactions showed that complexes Ir-Ph-d₅, Ir-D₃ and Ir-D₄ were no longer present in solution.

While exhaustive deuteration is desirable in some situations, mild, selective deuteration has some interest for drug discovery and evaluation.6, 8 The data in Table 1 indicates that, under conditions where Ir-D₄ dominates, deuteration is emphasized at the more sterically accessible sites (see Entry 9). We therefore examined HIE with the substrates in Figure 4 under these conditions (blue data). Using these conditions, good selectivity is possible with compounds containing directing groups and less accessible C_{sp2}-H sites. While fluorobenzene still showed almost quantitative deuterium incorporation, naphthalene, 2,6lutidine and N,N-dimethylbenzamide showed higher levels of deuteration at accessible sites relative to less accessible ones. Catalytic HIE of aniline had a slightly greater preference for -NH and ortho- sites. The increased propensity of the iridium catalyst to bind at the more strongly donating -NH site likely resulted in this mild enhancement. While selectivity was observed in phenol, results were almost identical to the exhaustive conditions with the -OH and ortho- positions being deuterated to 42%

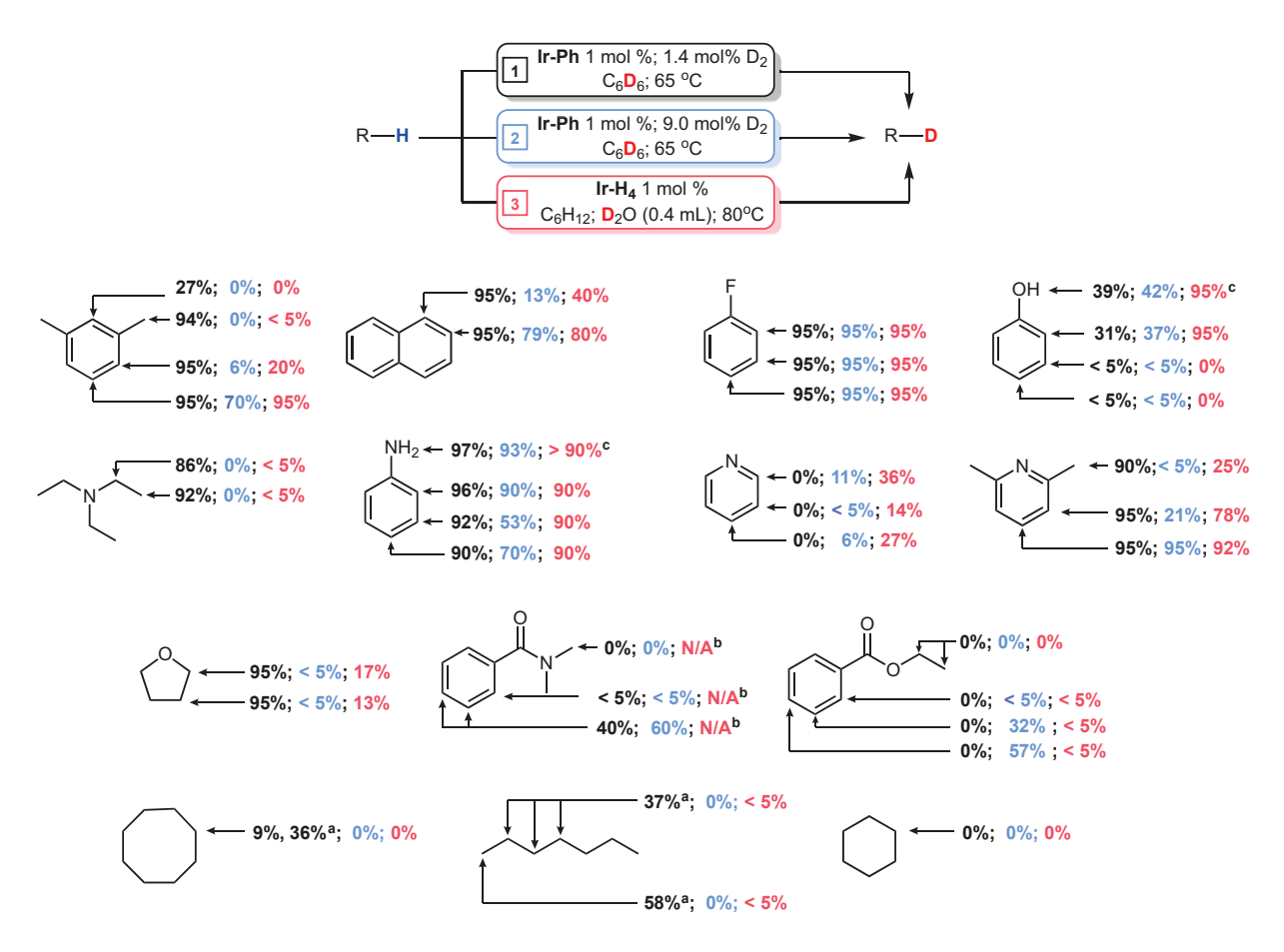


Figure 4. Distribution of deuterium throughout various substrates following reactions using C_6D_6 or D_2O as a deuterium source. Yields marked black and blue were obtained from reactions with substrates (0.38 mmol) using Ir-Ph (1 mol%) activated by 1.4 mol% (black) or 9.0 mol% (blue) of D_2 gas in C_6D_6 (1.0 mL) and heating to 65 °C for 24 hours. Yields marked in red were obtained from reactions with substrates (0.38 mmol) using Ir-H₄ (1 mol%) in C_6H_{12} (0.750 mL) and heating to 80 °C in the presence of D_2O for 24 hours. Conversion was measured via ¹H NMR using cyclohexane as an internal standard. For representative spectra for m-xylene, see Figures S22-S24 in the ESI. ^a Conversion after 5 days at 65 °C. ^b Reaction was not performed due to poor solubility. ^c These positions are deuterated via uncatalyzed exchange in D_2O .

and 37%, respectively. More surprisingly, deuteration for ethyl benzoate and pyridine became possible. Ethyl benzoate was significantly deuterated at both the meta- and para- positions while pyridine showed low level deuteration at all sites. For both pyridine and ethyl benzoate, the greater amount of $Ir-D_4$ may stave off immediate catalyst decomposition by providing increased levels of molecular D_2 present in solution which help prevent these substrates from strongly binding to the iridium center. Under these conditions deuteration at C_{sp3} -H sites was essentially shut down in all cases.

The use of C_6D_6 as a deuterium source is convenient but in an effort to carry out the reaction with a more economical source of D, we took advantage of the high tolerance of the iridium complexes of this PCP framework towards water and explored the use of D_2O as a deuterating agent for the HIE reaction. Table S2 gives the results of a short optimization study, again using meta-xylene as a substrate, and the red data in Figure 4 shows the results HIE using D_2O with Ir- H_4 under static vacuum as the catalyst precursor. To solubilize the iridium species, reactions were performed in a biphasic mixture of D_2O and cyclohexane. 31 , 33 For meta-xylene, H/D exchange occurred in trace amounts at the benzyl position,

20% at the 4 and 6 positions and quantitatively at the 5 position. Deuteration of the other substrates in Figure 4 using D₂O gave broadly similar results to those obtained under the "selective" conditions giving rise to the blue data, with a few notable differences. Fluorobenzene was again exhaustively deuterated while naphthalene and 2,6-lutidine had deuterium unevenly distributed throughout the arene systems. Aniline was deuterated almost quantitively in all positions while deuteration in phenol was greatly enhanced to 95%, although limited to the ortho and -OH sites. Deuterium levels in pyridine were found to be slightly higher than in the previous attempts but again catalysis was hampered by catalyst degradation (detected via 31P{1H} NMR). Aliphatic hydrocarbons were found to be mostly unreactive though trace H/D exchange had occurred at the terminal methyl positions of *n*-heptane. Unlike the results produced using Ir-Ph and 9 mol% D₂ with benzened₆, H/D exchange was found to be possible in both triethylamine and THF, albeit in low levels.

On a preparative scale, these biphasic conditions can be used with neat substrates as summarized in Figure 5. Both benzene and fluorobenzene (8.3 mmol each) were deuterated

Figure 5. Distribution of deuterium throughout neat immiscible liquids following reactions using D₂O. Reactions were heated under static vacuum a 80 $^{\circ}$ C except for THF (100 $^{\circ}$ C with NaOH (6M) dissolved in D₂O) and (120 $^{\circ}$ C).

at all positions to 90% and 94%, respectively, with D_2O (305 mmol) at 80 °C using 1 mol% of Ir-H₄. Following extraction of the organic layers and distillation of the liquids, Ir-H₄ was recovered in excess of 90% and deuterated benzene and fluorobenzene were each isolated in about 80% yield. The experiments were repeated with the recovered Ir-H₄ and deuterium with minimal loss of catalyst performance, as shown in Figure 5.

Using a slightly modified methodology, both THF and nheptane were partially deuterated and isolated in good yields. Ir-H₄ was not soluble in THF/D₂O mixtures, so a 6M solution of NaOH in D₂O was employed to render the medium biphasic.⁶³ Heating Ir-H₄ (1 mol%) dissolved in neat THF (8.3 mmol) under static vacuum to 100 $^{\circ}\text{C}$ in the presence of a D_2O with NaOH (6M) solution resulted in both the 2 and 3 positions were deuterated to 74% and 65%, respectively. Lower temperatures produced significantly lower yields as did performing the reaction under 1 atmosphere of argon. Deuterated THF was isolated in an 84% yield via distillation and the catalyst was again recovered in 90% yield. NMR analysis of the recovered iridium material in THF revealed the mixture was composed of Ir-H₄, Ir-H₃ and Ir-OD (76%, 3% and 21%, respectively). All material was easily converted back to Ir-H₄ by placing the solution under 4 atmospheres of H2 gas. In order to partially deuterate n-heptane slightly higher temperature (120 °C) was required. After 24 hours the material was isolated and NMR analysis revealed n-heptane had been substantially deuterated to 63% at the terminal methyl positions and 28% among all methylene positions.

Conclusions

Since our initial report in 2012³⁵ on iridium complexes of the PC_{carbene}P framework, buttressed by robust aryl groups linking the arms of the pincer to the central carbene, the ligand design has evolved^{40, 43, 44} into the rigid, planar and highly electron-

fully regenerated

H

Ir
$$(Pr)_2$$

inactive stable catalyst precursor

H2

H2

N

(Pr)_2

H3

H4

Ir $(Pr)_2$

N

(Pr)_2

(Pr)_2

N

(Pr)_2

(Pr)_

Scheme 5. Summary of ligand design features and their implications for HIE activity in Ir-H₄.

donating ligand employed here to prepare and isolate Ir-H₄. Three features of this advanced ligand design make it a highly effective HIE catalyst system (Scheme 5). The electron richness of the ligand allows for the stabilization of the Ir-H4 form of the catalyst such that it is isolable, storable, and able to fully regenerate if the system is exposed to excess dihydrogen. However, loss of one equivalent of H₂ is facile, allowing for access to the Ir-H₂/Ir-H₃ manifold, which is moderately active as an HIE catalyst and able to effect selective deuteration of sterically accessible positions on some substrates. We propose that further removal of H₂, formally speaking, allows access to an even more active Ir-[]/Ir-H catalyst; this species, while not observed experimentally, is implied by the stoichiometry of the reactions that lead to its generation. This species is highly effective at activating a wide variety C-H and C-D bonds via oxidative addition, including bonds normally reticent towards activation. While highly reactive, this species is robust under HIE conditions by virtue of the electron richness of the ligand.

A second useful feature in this context, is the ability of these compounds to cooperatively move hydrogen atoms from metal to pincer carbene via a low barrier 1,2-shift. This increases their hydrogen capacity in each HIE active manifold while also providing a mechanism for opening coordination space for bond-activating interaction with C_6D_6/D_2O and substrate as is necessary for HIE. This also provides a low barrier path for the H/D scrambling that must occur in order to drive HIE reactions to completion. Finally, the third positive attribute is the rigidity of the ligand framework, as imposed by the aryl groups in the backbone and more crucially the linking Me_2C group. This design element imparts thermal stability and by avoiding undesirable catalyst deactivation pathways available to the unlinked variants. Furthermore, this rigidification also makes the 1,2-shift alluded to above more

facile by discouraging pyramidalization of the pincer ligand anchoring carbon atom. This has the effect of "flattening the curve" on the energy surface joining the $PC_{sp3}P$ (as in $Ir-H_2$ and Ir-II) and $PC_{carbene}P$ (e.g. $Ir-H_3$ and Ir-II) forms of the active species by making the C-H bond in the $PC_{sp3}P$ form weaker and rendering the overall HIE process more efficient. Thus, through advanced ligand design, we have developed a robust, recyclable catalyst for the selective or near exhaustive deuteration of a number of substrates, including on a preparative scale, under mild conditions and using C_6D_6 or D_2O as a deuterium source.

Experimental Section

General Considerations.

All compounds were stored, handled and manipulated, unless otherwise stated, using standard techniques in a VAC glovebox or on a double manifold high vacuum line under an atmosphere of argon purified via passage through an OxisorBW scrubber (Model 641-02 Matheson Gas Products). An M-Braun solvent purification system was used to dry npentane which was subsequently stored sodium/benzophenone ketal in a 500 mL thick-walled glass pressure flask. Benzene, benzene- d_6 , toluene, toluene- d_8 , THF d_8 and cyclohexane were dried over sodium/benzophenone ketal and stored under vacuum in a 100 mL thick-walled glass pressure flask. All dried solvents were degassed and vacuum distilled prior to use. Triethylamine, aniline, pyridine and 2,6lutidine were dried over CaH₂ and distilled prior to use. Fluorobenzene and ethyl benzoate were dried over 3 Å molecular sieves and filtered off. Methylcyclohexane- d_{14} , cyclohexane- d_{12} , cyclooctane, and n-heptane were purchased from Sigma-Aldrich and degassed via freeze-pump-thaw prior to use. Phenol, N,N-dimethylbenzamide and naphthalene were placed under 1 atmosphere of argon prior to use. H₂ (99.5%) and D₂ (99.98%) were purchased from Praxair and used without further purification. Iridium (III) chloride hydrate was purchased from Pressure Chemicals Inc. and used as received. [Ir(COE)₂Cl]₂ and Ir-Cl were prepared as previously reported.^{44,} 64 ^{1}H and $^{13}\text{C}\{^{1}\text{H}\}$ NMR chemical shifts were referenced to residual solvent protons and naturally abundant ¹³C resonances for all deuterated solvents.65 Chemical shift assignments are based on 1H , $^{31}P\{^1H\}$, $^{13}C\{^1H\}$, $^1H^{-1}H\text{-COSY}$, $^1H\text{-}$ ¹³C-HSQC and ¹H-¹³C HMBC NMR experiments performed on Bruker Ultrashield 400, Ascend-500, or Avance-600 MHz spectrometers using TopSpin version 3.2 software. X-ray crystallographic analyses were performed on a Nonius system equipped with a Bruker Apex-II CCD using samples coated in Paratone 8277 oil (Exxon) and mounted on a glass fibre. Elemental analyses were performed by staff of the Instrumentation Facility in the Department of Chemistry, University of Calgary.

Synthesis of Ir-OH.

To a 100 mL thick walled round bottomed pressure flask charged with CsOH \bullet H $_2$ O (0.866 g, 5.16 mmol) and a Teflon stir bar, Ir-CI (0.388 g, 0.516 mmol) dissolved in toluene (25 mL)

was added. The flask was sealed and heated to 120 °C. After stirring for 24 hours the green-brown solution had turned dark brown-red. This solution was cooled to room temperature and filtered through a pad of Celite® into a 50 mL round bottom flask. All volatiles were removed from the filtrate in vacuo and n-pentane (20 mL) was vacuum transferred into the flask at -78 °C. The flask was warmed to room temperature and the solution was stirred for 2 hours. All volatiles were removed in vacuo. A brown powder (0.301 g, 0.410 mmol) was isolated in 80% yield. Elemental Analysis Calcd. (%): C, 52.37; H, 7.00; N, 3.82. Found (average of 4 trials): C, 53.41; H, 7.25; N, 3.59. (the carbon value is high due to small amounts of unremovable toluene.) APCI-MS (M*+) for $C_{32}H_{51}IrN_2OP_2$: Calcd.: 734.3100. Found: 734.3070. 1 H NMR (500 MHz, C_6D_6) δ 6.70 (dvt, $^{4}J_{HH}$ = 2.3 Hz, J_{HP} = 3.7 Hz, 2H, ArH), 6.34 (d, $^{4}J_{HH}$ = 2.3 Hz, 2H, ArH), 3.64 (t, ${}^{2}J_{HP}$ = 3.8 Hz, 1H, Ir-OH), 2.95 (m, 4H, PCH(CH₃)₂, 2.36 (s, 12H, $N(CH_3)_2$), 1.65 (s, 6H (18H with $PCH(CH_3)_2$), --C(CH₃)₂-), 1.63 (dvt, ${}^{3}J_{HH}$ = 7.5 Hz, J_{HP} = 7.3 Hz, 12H (18H with - $C(CH_3)_2$ -), $PCH(CH_3)_2$), 1.40 (dvt, $^3J_{HH}$ = 7.1 Hz, J_{HP} = 7.1 Hz, 12H, PCH(CH₃)₂).¹³C{¹H} NMR (126 MHz, C₆D₆) δ 197.0 (t, ² J_{CP} = 2.2 Hz, Ir=C), 158.7 (vt, , J_{CP} = 18.8 Hz, ArC), 149.9 (vt, J_{CP} = 3.9 Hz, ArC), 142.5 (vt , J_{CP} = 20.0 Hz, ArC) 130.3 (vt, , J_{CP} = 7.8 Hz, ArC), 116.3 (s, ArCH), 114.4 (s, ArCH), 42.7 (s, -C(CH₃)₂-), 40.2 (s, $N(CH_3)_2$), 28.2 (s, $-C(CH_3)_2$ -), 25.3 (vt, $J_{CP} = 12.8 \text{ Hz}$, $PCH(CH_3)_2$), 20.0 (vt, $J_{CP} = 2.7 \text{ Hz}$, PCH(CH₃)₂), 19.7 (s, PCH(CH₃)₂).³¹P{¹H} NMR (203 MHz, C_6D_6) δ 51.9 (s).

Synthesis of Ir-H₄.

Method 1: To a 100 mL thick walled glass pressure vessel equipped with a Teflon stirbar, Ir-OH (0.196 g, 0.267 mmol) dissolved in benzene (15 mL) was loaded. The mixture was degassed via the freeze-pump-thaw method and placed under 4 atm. of H₂ gas. After stirring for 3 hours all volatiles were removed in vacuo resulting in a dark red-brown residue. To this *n*-pentane (25 mL) were added via vacuum transfer at -78 ^oC. The solution was warmed to room temperature and stirred for 20 minutes under 1 atm of H₂. The *n*-pentane was removed under high vacuum and a beige powder (0.188 g, 0.260 mmol) was isolated in 98% yield. Elemental Analysis Calcd. (%): C, 53.24; H, 7.68; N, 3.88. Found: C, 53.48; H, 8.11; N, 3.73. Method 2: To a 100 mL thick walled glass pressure vessel charged with NaOH (0.266 g, 6.65 mmol) and a Teflon stirbar, Ir-Cl (0.500 g, 0.665 mmol) dissolved in benzene (35 mL) was loaded. The mixture was degassed via the freeze-pump-thaw method and then placed under 4 atm. of H₂ gas. After stirring for 3 hours the now orange-yellow solution was degassed and filtered through a pad of Celite® in a glovebox. The filtrate was placed in a 50 mL round bottom flask and all volatiles were removed in vacuo. To the dark-red residue n-pentane (25mL) was vacuum transferred at -78 °C. The mixture was warmed to room temperature, placed under 1 atmosphere of H2 gas and stirred for 20 minutes. All volatiles were removed in vacuo and a beige powder (0.454 g, 0.627 mmol) was isolated in 94% yield. X-ray quality crystals were obtained by slowly cooling a supersaturated solution of Ir-H₄ in isopropanol from 50 ºC to 20 °C. Elemental Analysis Calcd. (%): C, 53.24; H, 7.68; N, 3.88. Found: C, 53.43; H, 7.88; N, 3.80. 1 H NMR (500 MHz, $C_{6}D_{12}$) δ

6.84 (d, ${}^4J_{HH}$ = 1.9 Hz, 2H, ArH), 6.48 (dvt, ${}^4J_{HH}$ = 1.9 Hz, J_{HP} = 4.0 Hz, 2H, ArH) , 5.52 (s, 1H, Ir-CH), 2.85 (s, 12H, N(CH₃)₂), 2.10 (m, 2H, PCH(CH₃)₂), 1.91 (m, 2H, PCH(CH₃)₂), 1.84 (s, 3H, -C(CH₃)₂-), 1.23 (s, 3H, -C(CH₃)₂, 1.16 (dvt, ${}^3J_{HH}$ = 7.9 Hz, J_{HP} = 7.4 Hz, 6H, PCH(CH₃)₂), 1.07 (m, 12H, PCH(CH₃)₂), 0.78 (dvt, ${}^3J_{HH}$ = 8.0 Hz, J_{HP} = 7.3 Hz, 6H, PCH(CH₃)₂), -10.32 (t, ${}^2J_{HP}$ = 10.7 Hz, 4H).¹³C{¹H} NMR (126 MHz, C₆D₁₂) δ 151.6 (vt, , J_{CP} = 15.4 Hz, ArC) 149.2 (vt, J_{CP} = 4.3 Hz, ArC), 145.2 (vt , J_{CP} = 7.4 Hz, ArC) 139.6 (vt, , J_{CP} = 24.4 Hz, ArC), 112.1 (s, ArCH), 111.6 (s, ArCH), 41.9 (s, N(CH₃)₂), 40.8 (s, -C(CH₃)₂-), 30.3 (s, -C(CH₃)₂-), 30.1 (vt, J_{CP} = 14.8 Hz, PCH(CH₃)₂), 25.0 (s, -C(CH₃)₂-), 23.1 (vt, J_{CP} = 16.7 Hz, PCH(CH₃)₂), 21.0 (s, Ir-CH), 20.2 (s, PCH(CH₃)₂), 20.2 (vt, J_{CP} = 2.2 Hz, PCH(CH₃)₂), 19.4 (vt, J_{CP} = 3.7 Hz, PCH(CH₃)₂), 18.0 (s, PCH(CH₃)₂). ³¹P{¹H} NMR (203 MHz, C₆D₁₂) δ 56.5 (s).

Synthesis of Ir-Ph.

To a 25 mL round bottom flask equipped with a Teflon stirbar, Ir-H₄ (0.180 g, 0.249 mmol) dissolved in benzene (10 mL) was added. The solution was stirred at room temperature in a glovebox and tert-butylethylene (0.105 g, 1.069 mmol) was added. After stirring for 10 minutes all volatiles were removed in vacuo. The dark green-brown residue was then sonicated in *n*-pentane (5 mL). The solid was then filtered through a fritted Büchner funnel and washed with n-pentane (3 x 2mL). A dark green powder (0.143 g, 0.180 mmol) was isolated in 73% yield. X-ray quality crystals were obtained from a saturated solution of Ir-Ph in n-pentane that was sealed at room temperature in a 20 mL scintillation vial for 1 week. Elemental Analysis Calcd. (%): C, 57.48; H, 6.98; N, 3.53. Found: C, 57.59; H, 6.99; N, 3.52. ¹H NMR (500 MHz, C_6D_6) δ 7.54 (t, $^3J_{HH}$ = 7.4 Hz, 2H, Ph-H), 7.14 (d, ${}^{3}J_{HH}$ = 7.3 Hz, 2H, Ph-H), 6.97 (t, ${}^{3}J_{HH}$ = 7.3 Hz, 1H, Ph-H), 6.74 (m, 2H, Ar-H), 6.25 (d, ${}^{4}J_{HH}$ = 2.2 Hz, 2H, Ar-H), 3.16 (m, 2H, $P(CH(CH_3)_2)$, 2.25 (s, 12H, $N(CH_3)_2$, 1.63 (s, 6H, - $C(CH_3)_2$), 1.40 (dvt, ${}^3J_{HH} = 7.0 \text{ Hz}$, ${}^3J_{HP} = 7.0 \text{ Hz}$ 12H, $PCH(CH_3)_2$), 1.35 (dvt, ${}^{3}J_{HH} = 7.9 \text{ Hz}$, ${}^{3}J_{HP} = 7.3 \text{ Hz}$ 12H, PCH(CH₃)₂). ${}^{13}C\{{}^{1}H\}$ NMR (126 MHz, C_6D_6) δ 221.1 (t, $^2J_{CP}$ = 4.0 Hz, C=Ir), 171.8 (vt, J_{CP} = 8.8 Hz, PhC-Ir), 157.7 (vt, J_{CP} = 19.2 Hz, ArC), 151.4 (vt, J_{CP} = 3.9 Hz, ArC), 147.3 (vt, J_{CP} = 17.9 Hz, ArC), 142.2 (vt, J_{CP} = 7.3 Hz, ArC), 140.2 (s, PhCH), 126.6 (s, PhCH), 120.8 (s, PhCH), 116.6 (s, ArCH), 113.7 (s, ArCH), 43.5 (s, -C(CH₃)₂-), 40.2 (s, N(CH₃)₂), 27.4 (s, $-C(CH_3)_2$ -), 24.3 (vt, $J_{CP} = 13.3$ Hz, $PCH(CH_3)_2$), 20.1 (vt, $J_{CP} = 2.4 \text{ Hz}, PCH(CH_3)_2), 19.3 \text{ (br s, PCH(CH_3)_2)}. ^{31}P\{^{1}H\} NMR$ (203 MHz, C_6D_6) δ 53.6 (s).

Generation of Ir-H₃.

To a J-Young tube charged with Ir-Ph (0.010 g, 0.025 mmol) dissolved in C_6H_6 (0.25 mL), Ir-H $_4$ (0.013 g, 0.037 mmol) in C_6H_6 (0.35 mL) was added dropwise over 5 minutes. The solution changed from dark green to a dark reddish brown color. Ir-H $_3$ is generated *in situ* and is unisolable. 1H NMR (500 MHz, C_6H_6 spiked with C_6D_{12}) δ 6.78 (m, Ar-H), 6.63 (d, $^4J_{HH}$ = 2.5Hz Ar-H), 2.58 (s, 12 H, N(CH $_3$) $_2$), 2.25 (m, 4 H, PCH(CH $_3$) $_2$), 1.63 (s, 6 H, C(CH $_3$) $_2$ -), 1.46 (dvt, J_{HP} = 7.5 Hz, PCH(CH $_3$) $_2$), 1.14 (m, PCH(CH $_3$) $_2$). 13 C{ 1H } NMR (126 MHz, C_6H_6 spiked with C_6D_{12}) δ 245.0 (br s, C=Ir); 152.4 (vt, J_{CP} = 19.8 Hz, ArC), 152.1 (vt, J_{CP} = 19.0 Hz, ArC), 150.4 (vt, J_{CP} = 3.3 Hz, ArC), 140.1 (vt, J_{CP} = 6.9 Hz, ArC), 115.4 (s, ArCH), 112.3 (s, ArCH), 41.3 (s, -C(CH $_3$) $_2$ -),

40.8 (s, N(CH₃)₂), 32.1 (s, -C(CH₃)₂-), 27.3 (vt, J_{CP} = 15.6 Hz, PCH(CH₃)₂), 21.9 (s, PCH(CH₃)₂), 19.8 (s, PCH(CH₃)₂). ³¹P{¹H} NMR (203 MHz, C₆D₆) δ 66.4 (s).

Preparation of Stock Solutions.

Solution A. Complex Ir-Ph (0.060 g, 0.076 mmol, 0.015 M) was dissolved with benzene- d_6 in a volumetric flask (5 mL). Solution B. Cyclohexane was added to a volumetric flask (5 mL) containing complex Ir-H₄ (0.068 g, 0.094 mmol, 0.019 M) and cyclohexane- d_{12} (0.550 g, 5.07 mmol, 1.15 M). Solution C. Cyclohexane was added to a volumetric flask (1 mL) containing Solution B (0.450 mL) and substrate (0.85 mmol).

General Procedure for Deuteration of Substrates in C₆D₆.

Stock *Solution A* (0.80 mL) was added to a glass reaction tube (length: 8.5 cm length, inner diameter: 1.5 cm) equipped with a Teflon stirbar. The flask was sealed with a rubber stopper and 1.4 mol% (0.405 mL, 0.017 mmol at 20 °C) or 9 mol% (2.6 mL, 0.11 mmol) D_2 gas was injected into the flask. After stirring for 10 minutes at 20 °C, the solution (0.250 mL, 0.0038 mmol of [Ir]) was injected into a J-Young tube containing substrate (0.38 mmol), cyclohexane (0.046 mmol) and benzene- d_6 (0.75 mL). The solution was heated to 65 °C for 24 hours and conversion was measured using cyclohexane as an internal standard. Cyclohexane was monitored without the use of an internal standard; no detectable traces of deuterium incorporation were visible using 1 H, 2 H or 13 C{ 1 H} NMR.

General Procedure for Deuteration of Substrates in Cyclohexane with D_2O .

Stock Solution C (0.450 mL) was added to a pressure tube (10 mL) charged with cyclohexane (0.300 mL), argon sparged D₂O (0.4 mL, 0.022 mmol) and a Teflon stirbar. Another sample was prepared by placing stock Solution C (0.450 mL) and cyclohexane (0.300 mL) in an NMR tube; this sample was used as a starting material reference. The flask was sealed under argon (1 atm.) with a Teflon valve and heated to the appropriate temperature. After 24 hours the organic phase was carefully transferred to an NMR tube under argon without exposure to air. Conversion was measured via ¹H NMR using the cyclohexane signal as the internal standard. The reference samples containing water miscible/soluble compounds (THF, triethylamine, 2, 6-lutidine, pyridine, aniline and phenol) were extracted with D₂O prior to running NMR. The ¹H NMR spectra of the organic phases for these samples were compared to the organic phases of the reaction mixtures to measure conversion. Aliquots of the D₂O fractions (0.2 mL) for both the reference and reaction mixtures were also taken and added to separate NMR samples containing D₂O (0.4 mL) and DMSO (10 uL). The ¹H NMR spectra for these samples indicated comparable levels of deuteration were present in the D₂O

General Procedure for Deuteration of Neat Benzene, Fluorobenzene and n-heptane with D_2O .

Substrate (8.31 mmol) was loaded into a pressure tube (10 mL) charged with Ir-H₄ (0.060 g, 0.083 mmol) and a Teflon stirbar. Argon sparged D₂O (6.0 mL, 330 mmol) was carefully added to the reaction flask under a steady flow of argon. The vessel was

sealed with a Teflon valve and heated to 80 °C for 24 hours. The flask containing *n*-heptane was freeze-pump-thawed three-fold and heated to 120 °C under static vacuum for 24 hours. Organic phases were extracted under a flow of argon *via* syringe and liquids were distilled under reduced pressure from the iridium catalyst. Benzene was isolated in 81% yield (0.561 g, 6.72 mmol) with 90% deuterium incorporation. Fluorobenzene was isolated in 82% yield (0.725 g, 6.81 mmol) with 94% deuterium incorporation at all positions. *n*-heptane was isolated in 88% yield (0.791 g, 7.40 mmol) with 63% deuterium at the terminal methyl positions and 28% deuterium incorporation throughout the methylene position.

Deuteration of THF with D₂O.

THF (0.600 g, 8.32 mmol) was added to a pressure tube (10 mL) charged with Ir-H₄ (0.060 g, 0.083 mmol) and a Teflon stirbar. Argon sparged D₂O (6 mL) containing NaOH (1.45 g, 36.3 mmol, 6 M) was added to the flask under a flow of argon. The mixture was freeze-pump-thawed three-fold and sealed under static vacuum. After heating at 100° C for 24 hours the organic phase was extracted under a flow of argon *via* syringe and distilled under reduced pressure from the iridium catalyst. Deuterated THF was isolated in 84% yield (0.547 g, 7.03 mmol) with deuterium incorporated in 74% and 65% at the 2 and 3 positions, respectively.

Conflicts of interest

There are no conflicts to declare.

Acknowledgements

Funding for this work was provided by NSERC of Canada (Discovery Grant) and the Canada Research Chair secretariat (Tier I CRC 2013-2020) to W.E.P. Author J.D.S thanks NSERC of Canada for PGSD Scholarship support. D.H.E acknowledges the United States National Science Foundation Chemical Structure, Dynamics, and Mechanisms B (CSDM-B) Program for support under award CHE 1952420. We thank Brigham Young University and the Office of Research Computing, especially the Fulton Supercomputing Lab. G. D. thanks the BYU Department of Chemistry and Biochemistry for undergraduate research awards.

Notes and references

- J. Yang, Deuterium: Discovery and Applications in Organic Chemistry, Elsevier, Amsterdam, 2016.
- J. L. Garnett and R. J. Hodges, J. Am. Chem. Soc., 1967, 89, 4546-4547.
- J. L. Garnett and R. S. Kenyon, J. Chem. Soc. D, 1971, 1227-1228.
- 4. N. F. Goldshleger, M. B. Tyabin, A. E. Shilov and A. A. Shteinman, *Zh. Fiz. Khim.*, 1969, **43**, 1222-+.
- A. E. Shilov and A. A. Shteinman, Coord. Chem. Rev., 1977,
 24. 97-143.
- 6. T. G. Gant, J. Med. Chem., 2014, **57**, 3595-3611.

- R. Pony Yu, D. Hesk, N. Rivera, I. Pelczer and P. J. Chirik, Nature, 2016, 529, 195-199.
- J. Atzrodt, V. Derdau, W. J. Kerr and M. Reid, Angew. Chem. Int. Ed. Engl., 2018, 57, 1758-1784.
- T. Junk and W. J. Catallo, Chem. Soc. Rev., 1997, 26, 401-406.
- J. Atzrodt, V. Derdau, T. Fey and J. Zimmermann, Angew. Chem. Int. Ed. Engl., 2007, 46, 7744-7765.
- J. Atzrodt, V. Derdau, W. J. Kerr and M. Reid, Angew. Chem. Int. Ed. Engl., 2018, 57, 3022-3047.
- R. H. Crabtree, H. Felkin and G. E. Morris, J. Organomet. Chem., 1977, 141, 205-215.
- A. H. Janowicz and R. G. Bergman, J. Am. Chem. Soc., 1982, 104, 352-354.
- A. H. Janowicz and R. G. Bergman, J. Am. Chem. Soc., 1983, 105, 3929-3939.
- B. A. Arndtsen and R. G. Bergman, Science, 1995, 270, 1970-1973.
- J. T. Golden, R. A. Andersen and R. G. Bergman, J. Am. Chem. Soc., 2001, 123, 5837-5838.
- S. R. Klei, J. T. Golden, T. D. Tilley and R. G. Bergman, J. Am. Chem. Soc., 2002, 124, 2092-2093.
- G. N. Nilsson and W. J. Kerr, J. Labelled Comp. Radiopharm., 2010, 53, 662-667.
- S. R. Klei, T. D. Tilley and R. G. Bergman, *Organometallics*, 2002, 21, 4905-4911.
- M. B. Skaddan, C. M. Yung and R. G. Bergman, *Org. Lett.*, 2004, 6, 11-13.
- C. M. Yung, M. B. Skaddan and R. G. Bergman, J. Am. Chem. Soc., 2004, 126, 13033-13043.
- L. L. Santos, K. Mereiter, M. Paneque, C. Slugovc and E. Carmona, New J. Chem., 2003, 27, 107-113.
- J. L. Rhinehart, K. A. Manbeck, S. K. Buzak, G. M. Lippa, W.
 W. Brennessel, K. I. Goldberg and W. D. Jones, Organometallics, 2012, 31, 1943-1952.
- 24. S. H. Lee, S. I. Gorelsky and G. I. Nikonov, *Organometallics*, 2013, **32**, 6599-6604.
- G. van Koten and D. Milstein, eds., Topics in Organometallic Chemistry: Organometallic Pincer Chemistry, Springer, Heidelberg, 2013.
- D. Morales-Morales, Pincer Compounds: Chemistry and Applications, Elsevier, Amsterdam, 2018.
- A. Kumar, T. M. Bhatti and A. S. Goldman, *Chem. Rev.*, 2017, 117, 12357-12384.
- N. A. Eberhardt and H. Guan, Pincer Compounds: Chemistry and Applications, Elsevier, Amsterdam, 2018.
- R. Tanaka, M. Yamashita and K. Nozaki, J. Am. Chem. Soc., 2009, 131, 14168-14169.
- M. H. G. Prechtl, M. Hoelscher, Y. Ben-David, N. Theyssen,
 D. Milstein and W. Leitner, Eur. J. Inorg. Chem., 2008,
- 31. M. H. G. Prechtl, M. Hölscher, Y. Ben-David, N. Theyssen, R. Loschen, D. Milstein and W. Leitner, *Angew. Chem. Int. Ed. Engl.*, 2007, **119**, 2319-2322.
- 32. J. Zhou and J. F. Hartwig, *Angew. Chem. Int. Ed. Engl.*, 2008, **47**, 5783-5787.
- 33. V. M. Iluc, A. Fedorov and R. H. Grubbs, *Organometallics*, 2011, **31**, 39-41.
- 34. A. V. Polukeev, R. Marcos, M. S. G. Ahlquist and O. F. Wendt, *Organometallics*, 2016, **35**, 2600-2608.
- R. J. Burford, W. E. Piers and M. Parvez, *Organometallics*, 2012, **31**, 2949-2952.

- C. C. Comanescu and V. M. Iluc, *Organometallics*, 2014,
 33, 6059-6064.
- S. Sung and R. D. Young, *Dalton Trans.*, 2017, 46, 15407-15414.
- 38. P. Cui and V. M. Iluc, Chem. Sci., 2015, 6, 7343-7354.
- S. Sung, Q. Wang, T. Krämer and R. D. Young, *Chem. Sci.*, 2018, 9, 8234-8241.
- L. E. Doyle, W. E. Piers and J. Borau-Garcia, J. Am. Chem. Soc., 2015, 137, 2187-2190.
- 41. C. Yoo and Y. Lee, *Angew. Chem. Int. Ed.*, 2017, **56**, 9502-9506
- D. Sahoo, C. Yoo and Y. Lee, J. Am. Chem. Soc., 2018, 140, 2179-2185.
- J. D. Smith, J. R. Logan, L. E. Doyle, R. J. Burford, S. Sugawara, C. Ohnita, Y. Yamamoto, W. E. Piers, D. M. Spasyuk and J. Borau-Garcia, *Dalton Trans.*, 2016, 45, 12669-12679.
- J. D. Smith, E. Chih, W. E. Piers and D. M. Spasyuk, *Polyhedron*, 2018, **155**, 281-290.
- J. D. Smith, J. Borau-Garcia, W. E. Piers and D. Spasyuk, Can. J. Chem., 2016, 94, 293-296.
- L. E. Doyle, W. E. Piers, J. Borau-Garcia, M. J. Sgro and D. M. Spasyuk, *Chem. Sci.*, 2016, 7, 921-931.
- E. A. LaPierre, W. E. Piers, D. M. Spasyuk and D. W. Bi, Chem. Comm., 2016, 52, 1361-1364.
- 48. E. A. LaPierre, W. E. Piers and C. Gendy, *Dalton Trans.*, 2018, **47**, 16789-16797.
- C. C. Comanescu and V. M. Iluc, Chem. Commun., 2016, 52, 9048-9051.
- L. E. Doyle, W. E. Piers and D. W. Bi, *Dalton Trans.*, 2017,
 46, 4346-4354.
- 51. E. A. LaPierre, W. E. Piers and C. Gendy, *Organometallics*, 2018, **37**, 3394-3398.
- 52. S. Sung, T. Joachim, T. Krämer and R. D. Young, Organometallics, 2017, 36, 3117-3124.
- 53. H. Tinnermann, S. Sung, B. A. Cala, H. J. Gill and R. D. Young, *Organometallics*, 2020, **39**, 797-803.
- 54. R. J. Burford, W. E. Piers, D. H. Ess and M. Parvez, *J. Am. Chem. Soc.*, 2014, **136**, 3256-3263.
- P. J. Desrosiers, L. Cai, Z. Lin, R. Richards and J. Halpern, J. Am. Chem. Soc., 1991, 113, 4173-4184.
- T. J. Hebden, K. I. Goldberg, D. M. Heinekey, X. Zhang, T. J. Emge, A. S. Goldman and K. Krogh-Jespersen, *Inorg. Chem.*, 2010, 49, 1733-1742.
- 57. F. Maseras, A. Lledós, M. Costas and J. M. Poblet, Organometallics, 1996, 15, 2947-2953.
- 58. S. Gründemann, H.-H. Limbach, G. Buntkowsky, S. Sabo-Etienne and B. Chaudret, *J. Phys. Chem. A*, 1999, **103**, 4752-4754.
- 59. D. Devarajan and D. H. Ess, *Inorg. Chem.*, 2012, **51**, 6367-6375
- A. V. Polukeev, R. Marcos, M. S. G. Ahlquist and O. F. Wendt, *Chem. Sci.*, 2015, 6, 2060-2067.
- A. V. Polukeev, R. Marcos, M. S. G. Ahlquist and O. F. Wendt, Chem. Eur. J., 2016, 22, 4078-4086.
- R. Corberan, M. Sanau and E. Peris, J. Am. Chem. Soc., 2006, 128, 3974-3979.
- Y. Xie, F. Yu, Y. Wang, X. He, S. Zhou and H. Cui, Fluid Phase Equilib., 2019, 493, 137-143.
- 64. J. L. Herde, J. C. Lambert, C. V. Senoff and M. A. Cushing, in *Inorganic Syntheses*, ed. G. W. Parshall, John Wiley & Sons, Inc., Hoboken, NJ, USA, 2007, pp. 18-20.

G. R. Fulmer, A. J. M. Miller, N. H. Sherden, H. E. Gottlieb, A. Nudelman, B. M. Stoltz, J. E. Bercaw and K. I. Goldberg, *Organometallics*, 2010, **29**, 2176-2179.

1

65.